Nonequilibrium occupancy of tail states and defects in *a*-Si:H: Implications for defect structure

G. Schumm, W. B. Jackson, and R. A. Street
Xerox Palo Alto Research Center, 3333 Coyote Hill Road, Palo Alto, California 94304
(Received 10 May 1993)

A detailed investigation of the electron and hole occupancy of tail states in undoped amorphous silicon (*a*-Si:H) as well as changes in the dangling-bond occupancy as a function of excitation intensity was carried out using light-induced electron-spin-resonance (LESR) measurements. For very thick films the band-tail electron and hole densities are not proportional. Over a wide range of excitation conditions the excess hole density is constant, suggesting the presence of charged defects with a density that is 5–10 times larger than the neutral defect density in annealed or as-grown *a*-Si:H. Light soaking increases mainly the neutral defect density. The dependence of the excess hole density on film thickness and absorption profiles indicates that this effect is a bulk property, which may be masked in thinner films by the comparatively high interface defect density. Model calculations of nonequilibrium occupation statistics confirm the experimental results. For a defect distribution that includes charged defects, the calculations suggest a very small positive LESR signature of the dangling bond, in spite of the high density of charged defects in the material, as a necessary consequence of the asymmetries observed between electron and hole capture rates and tail-state distributions. The calculations demonstrate that the lack of this signature does not imply a defect structure that contains predominantly neutral defects.

I. INTRODUCTION

According to the most widely accepted model for the defect structure in amorphous silicon, the density of gap states in undoped *a*-Si:H is dominated by a single band of neutral dangling-bond (DB) states with a comparatively large effective correlation energy. On the other hand, theoretical work based on thermodynamic equilibration,[1] specifically between weak and dangling bonds,[2–4] or based on potential fluctuations,[5] suggests that in spite of a positive correlation energy most DB's may be in the charged state, forming two independent bands of charged defects separated by the Fermi level. In both approaches, the ratio of charged to neutral defect density depends on the model parameters, in particular, on the assumed effective correlation energy in relation to the width of potential fluctuations[5] or the energetic width of available defect creation sites.[2] In this paper, dark- and light-induced electron-spin resonance measurements are invoked to determine the relative density of charged to neutral dangling bonds in device-grade undoped *a*-Si:H.

In both doped and undoped amorphous silicon three distinct electron-spin resonance absorption lines can usually be observed. One line with a g value of 2.0055 and a width of 7.5 G is attributed to the neutral singly occupied silicon dangling bond, the other two lines, with $g=2.0043$ and 2.01, observed only in light-induced electron-spin resonance (LESR) or doped material, have been ascribed to electrons in the conduction-band tail and holes in the valence-band tail. In early LESR studies, electron and hole absorption lines of undoped *a*-Si:H were found to be of roughly equal densities[6] with no discernable LESR signature of the dangling bond, suggesting that only an insignificant fraction of the DB defects are charged in undoped material. The proportionality between optical subgap absorption and spin density,[7] together with the temperature independence of the dark spin density,[8] led to the widely accepted conclusion that the dominant defect in undoped *a*-Si:H is the singly occupied, neutral, paramagnetic dangling bond with a positive effective correlation energy.

Recent, more detailed and accurate comparisons of absorption data and spin density have shown systematic deviations from proportionality.[9,10] Changes in the ratio of electron to hole LESR absorption lines have been reported, when comparing band to band with ir excitation[11] or when comparing as-grown with light-soaked samples.[12] Deconvolution of LESR signals, while accounting for surface defects, indicates a significant number of charged defects in the bulk of undoped *a*-Si:H.[13] In addition, the defect structure, as elucidated by the electrical properties of the material, does not show an altogether satisfactory agreement with the above conclusion. For instance, the lack of proportionality between photoconductivity and spin density[14] points to additional gap states acting as recombination centers. Another puzzling feature of undoped *a*-Si:H is the lack of any LESR signature of the DB.

A careful study of the three line intensities over wide ranges of temperature and illumination intensity should clarify this issue, but so far has not been reported, probably because of experimental difficulties. Applying extensive averaging procedures to increase the signal-to-noise ratio and using very thick films, we have obtained quantitative data about the nonequilibrium occupancy of tail and defect states in device-grade undoped *a*-Si:H for various excitation conditions. This allows us to derive the number of charged and neutral defects and to estimate the energetic positions of the various defect bands. In Sec. III, the occupation statistics are calculated using a simple model with recombination through tail states and correlated defect transition levels. Features such as the

0163-1829/93/48(19)/14198(10)/$06.00

missing dangling-bond LESR signature in undoped *a*-Si:H are addressed.

II. LESR MEASUREMENTS

A. Experimental details

Standard, device-grade undoped *a*-Si:H films from 0.3 to 15 μm thickness were deposited on quartz, on glass, and on Cr-coated quartz under identical growth conditions. Dark spin areal densities for the 0.3-μm film were 1.9×10^{12} cm^{-2}, equivalent to a bulk density of 6.5×10^{16} cm^{-3}, and for the 15-μm film 4.8×10^{12} cm^{-2}, equivalent to a bulk density of 3.2×10^{15} cm^{-3}. Subtracting the 1.9×10^{12} cm^{-2} surface and/or interface defects yields a bulk spin density of $\sim2\times10^{15}$ cm^{-3} for the thick film.

For LESR measurements white light from a halogen lamp was filtered by a 900-nm cutoff filter and additional filters to achieve desired absorption profiles and generation rates. Measurements were carried out from 32 K to room temperature and over five orders in generation rate.

To achieve a sufficient signal-to-noise ratio, up to 1000 consecutive field scans were numerically averaged. Typical scan times were 1–2 min. No further smoothing of the data was performed. For LESR spectra the dark signal was subtracted from the light-induced signal. Above 120 K the relaxation times were sufficiently short, so that extended averaging could be done by alternating scans under illumination and in the dark. For lower temperatures, first the dark spectra, then the spectra under illumination, were taken, each one with a number of scans that gave sufficient accuracy at a given signal intensity.

At each temperature, varying the microwave power over three orders of magnitude and checking for the expected square-root dependence ensured that the signal intensity was not affected by microwave saturation. While the absolute calibration of ESR data regarding spin densities may not be better than a factor 2–3, our conclusions are all based on relative numbers, such as the ratios of light-induced electron and hole spin densities, and those in comparison with the neutral DB densities in the dark. These values are considered to be accurate within 10–20 % relative error.

B. Dependence on excitation intensity

Figure 1 shows LESR absorption derivative spectra obtained from the 15-μm film on the Cr-coated substrate. The four spectra were taken for excitation intensities and temperatures giving roughly an order of magnitude variation in the hole density, decreasing from $p_t=3\times10^{17}$ cm^{-3} for the top spectra to 5.4×10^{16} for the bottom one. For better comparison, all curves have been rescaled to give equal amplitudes for the hole (h) lines. Even casual inspection of line heights shows that, as the hole density drops, the electron density drops faster, indicating a distinct disproportionality between electron and hole densities.

Accurate values for electron and hole densities at the various excitation conditions were obtained by fitting the derivative spectra as well as the integrated absorption spectra with a superposition of two Gaussian functions.

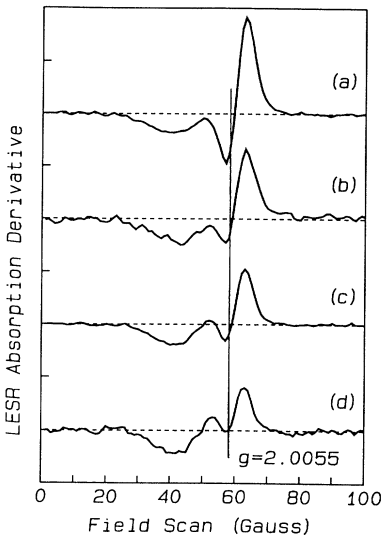

FIG. 1. LESR derivative spectra of an undoped 15-μm *a*-Si:H film for various illuminations and temperatures. (a) $T=32$ K, microwave power $P=8$ μW, white light, $p_t=3.3\times10^{17}$ cm^{-3}. (b) $T=32$, $P=8$ μW, residual signal after illumination, $p_t=8.8\times10^{16}$ cm^{-3}. (c) $T=95$ K, $P=125$ μW, white light, $p_t=7.8\times10^{16}$ cm^{-3}. (d) $T=95$ K, $P=125$ μW, red light, $p_t=5.2\times10^{16}$ cm^{-3}. The spectra have been adjusted to give equal amplitudes for the hole lines.

All lines for a given temperature and different excitation energies were fit with one set of parameters for the linewidth and position, allowing only the line heights to vary. The linewidth and position change little with temperature. The values are summarized in Table I. Generally, very good fits could be obtained. An example of the fit quality is shown in Fig. 2 for the spectra of Fig. 1(c), with an intermediate hole density $p_t=7.8\times10^{16}$ cm^{-3}. At this or higher intensities the hole and electron absorption could be determined with less than 10% relative error. Once the linewidth of the h line is known, the ratio of the e- to h-line intensity may also be directly read from the derivative spectra with good accuracy according to the relation

$$\frac{I_{h\ \mathrm{line}}}{I_{e\ \mathrm{line}}}=\frac{I_{pt}}{I_{nt}}\left[\frac{\Delta H_{pt}}{\Delta H_{nt}}\right]^2, \tag{1}$$

where I_{pt}, I_{nt} are the line heights and $\Delta H_{pt}, \Delta H_{nt}$ are the peak-to-peak widths of the hole and electron derivative spectra, respectively.

TABLE I. g value and linewidth of LESR electron and hole lines.

	g value		Linewidth (G)	
T(K)	Holes	Electrons	Holes	Electrons
32	~2.010	2.043	19±0.5	6.5
85–95	~2.011	2.043	17.5±0.5	6
165	~2.009	2.043	15±0.5	5.5

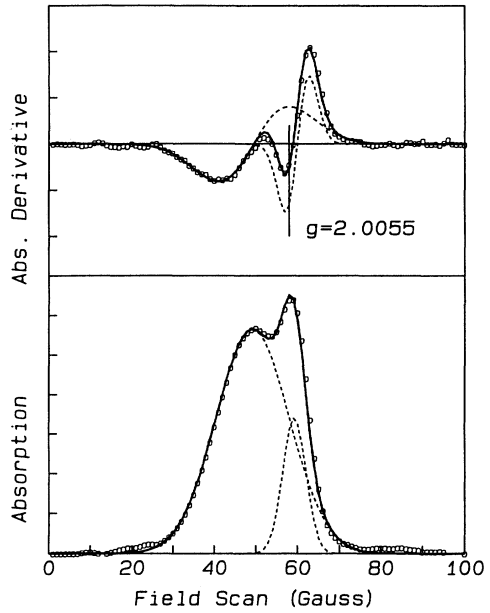

FIG. 2. Gaussian line fits to the spectrum of Fig. 1(c). Dashed curves are the electron and hole lines with fit parameters in Table I. Fits give a hole to electron spin density of ~5:1.

The data of Fig. 1 were taken for an intermediate light-soaked stage of the sample corresponding to a dark spin density $N_s = 1.1 \times 10^{16}$ cm^{-3}. Similar changes in the spectra have been found in the annealed sample with $N_s = 3.2 \times 10^{15}$ cm^{-3} and after light soaking to $N_s = 3.2 \times 10^{16}$ cm^{-3}. Figure 3 summarizes these results. Up to the highest intensities the hole density is larger than the apparent electron density n_s, with a clear deviation from proportionality towards lower densities. At high intensities all data seem to approach proportionality with $p_t \approx c_1 n_s$, where $c_1 \approx 2$–2.5 and n_s is the electron-spin density.

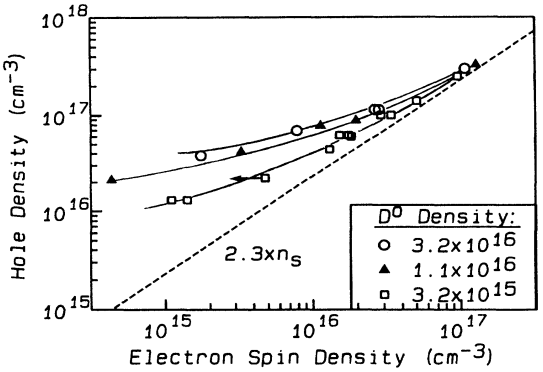

FIG. 3. Hole density vs electron-spin density n_s of the 15-μm sample in the annealed and two light-soaked states with indicated dark spin densities, for various excitation intensities and temperatures.

C. Electron-spin density and total electron density

At sufficiently high excitation intensity, where the carriers trapped in the band tails dominate the total charge, charge neutrality requires an equal number of band-tail electrons and band-tail holes, $p_t \approx n_t$. A number of possible effects may contribute to the apparent lower electron-spin density n_s, compared to the total electron density n_t. One reason may be the rather small correlation energy of conduction-band-tail states leading to spin coupling of the band-tail electrons, as inferred from the temperature dependence of the electron line in n-type material.[15–17] In this case, only a temperature-dependent fraction of singly occupied tail states n_s is observed where the total number of electrons is $n_t = c_1(T) n_s$. Figure 4 shows a normalized plot of $n_s(T)$ measured on a powder sample of phosphorus-doped a-Si:H deposited at 10^{-4} gas phase doping level, together with the calculated fraction of unpaired electrons in thermal equilibrium, assuming conduction-band-tail correlation energies between 10 and 30 meV and an exponential conduction-band-tail slope of 25 meV. The data suggests a correlation energy of about 20 meV, which yields $c_1(T) = 2.3$ at 32 K, in agreement with the proportionality constant inferred from our LESR measurements. Of course, other combinations of tail slope and correlation energy give similar fits, but the effect on $c_1(T)$ in the temperature range of interest is very small and does not affect the LESR results derived in the following. For doping levels of 10^{-2} and above, deviations from the monotonic increase of n_s with T are found.[15–17] The origin of these deviations is unclear, but increased coupling with dopant states might be a reason.

The LESR spectra were deconvoluted using Gaussian functions for the e and h line, an assumption which is not necessarily valid, although the Gaussian functions generally gave very good fits. The use of other line shapes affects the derived ratios of e to h lines only to a small extent. The assumed line shape primarily affects the proportionality constant that is observed for high excitation intensities. It has, however, little effect on the observed

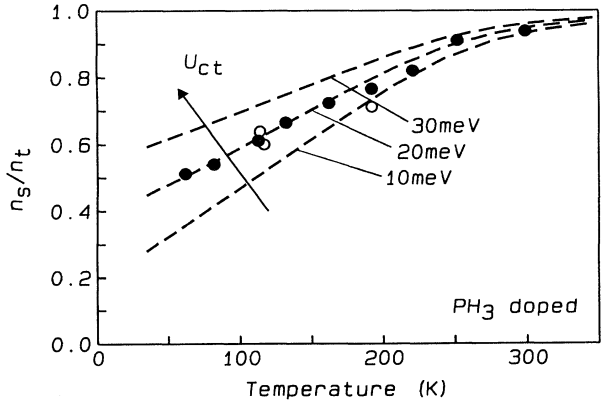

FIG. 4. Temperature dependence of the normalized electron-spin density for a lightly doped powder sample and calculated fraction of singly occupied conduction-band tail states assuming an exponential tail slope of 25 meV and correlation energies $U_{ct} = 10$–30 meV.

deviation from proportionality at low intensities.

Lack of proportionality between the *e*- and *h*-line intensity may arise from the possibility that spin pairing depends on the signal intensity. For instance, a more efficient spin pairing at lower light intensities could explain the apparent larger decrease of the *e* line. However, due to increasing localization one expects larger correlation energies for the deeper tail states, and hence less spin pairing for the more deeply trapped electrons. In this case, the *e*-line intensity should approach the *h*-line intensity at lower excitation intensities, in contrast to the observations, rendering it very unlikely that spin pairing causes the observed lack of proportionality. It is perhaps surprising that under illumination and at low temperatures spin pairing can be observed at all. However, under steady-state illumination, those conduction-band-tail states that are sufficiently isolated and deep to retain a captured electron will most likely capture a second electron and thus pair up their spin.

The possibility of microwave saturation and passage effects is also of concern. In principle, the increase of the electron recombination lifetime τ towards lower excitation intensities could lead to a stronger saturation, if τ is smaller than or comparable to the spin-lattice relaxation time T_1. However, even for the *e* line of the *n*-type sample in the dark we were not able to detect saturation at the microwave powers and temperatures used for the LESR experiment. The above argument suggests that under illumination there is less saturation for a given microwave power. Saturation effects in our LESR data are therefore very unlikely. Variation of field scan times from 0.5 to 16 min and field modulation frequencies from 100 Hz to 100 kHz at selected temperatures and light intensities did not affect the line shapes, ensuring that passage conditions are not responsible for the observed changes in line shape.

To summarize, the LESR line shape, and therefore the ratio of the electron to hole signal intensity, depends primarily on the absolute signal intensity (p_t) and, to a smaller extent, on the metastable state of the sample (annealed vs light soaked), but is essentially independent of the experimental conditions, i.e., the combination of excitation intensity and temperature leading to a given electron and hole density as well as microwave power, field modulation frequency, and scan time. This result holds for the entire temperature range from 32 to 165 K, and is strong evidence that the lack of proportionality observed between the *e* and *h* line is not due to an experimental artifact related to the measurement conditions.

D. Charged defect density

Taking $c_1(T)$ of Fig. 4 into account, the total electron density $n_t = c_1 n_s$ approaches p_t at high excitation intensities. However, as shown in Fig. 5, a marked difference $\Delta N = p_t - n_t$ still exists at lower intensities. ΔN is nearly constant over two orders of magnitude change in n_t, indicating the presence of additional, negatively charged defects $N_{D^-} = \Delta N$ to compensate the charge of the excess hole density. A slight increase of these charged defects from 2×10^{16} to 4×10^{16} and 5×10^{16} cm^{-3} is observed

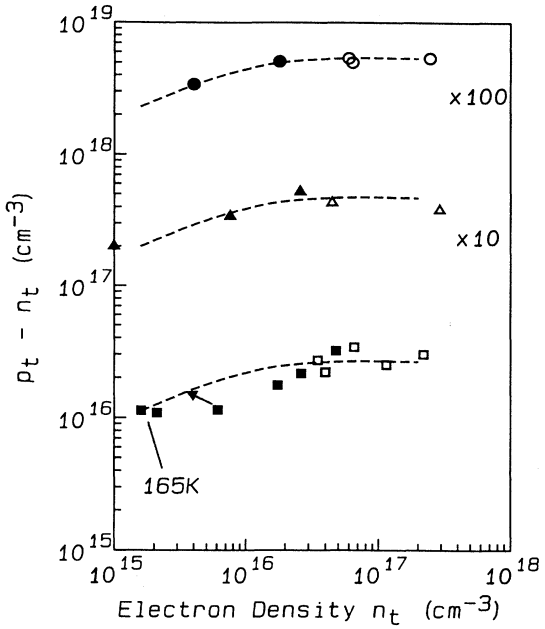

FIG. 5. Difference between hole and electron density from data of Fig. 3 and using $c_1(T)$ from Fig. 4. Empty symbols are from data taken at 32 K, full symbols at 85 and 95 K, indicated points at 165 K. Annealed: $N_s = 3.2\times10^{15}$ cm^{-3}, $p_t - n_t = 2.5\times10^{16}$ (squares); light soaked: $N_s = 1.1\times10^{16}$, $p_t - n_t = 4\times10^{16}$ (triangles); light soaked: $N_s = 3.2\times10^{16}$, $p_t - n_t = 5\times10^{16}$ cm^{-3} (circles).

when degrading the sample from a dark spin density of 3×10^{15} cm^{-3} to 1.1×10^{16} and 3.2×10^{16} cm^{-3}, respectively. The corresponding ratio of charged to neutral defects $\Delta N/N_s$ decreases from about 7 in the annealed sample to 4 and 1.6 in the two light-soaked states. In the range of largest n_t and p_t the derived difference ΔN is sensitive to the exact value of c_1. However, towards smaller n_t, where most of our data are taken, the influence of c_1 on this difference becomes marginal, and the derived ΔN is quite accurate. In Fig. 3, due to the log-log scale over three orders of magnitude, the deviation from proportionality may not appear significant in the medium range, where $n_s \approx 10^{16}$. However, this is the range seen in Figs. 1(b) and 1(c) where the ratio of *h*- to *e*-line intensities increases from 2.3:1 to about 3.5:1–5:1, indicating deviations from proportionality by up to 50%. The range of lowest n_s, corresponding to Fig. 1(d), shows ratios in excess of 9:1.

In principle, the narrow LESR line may be a combination of both electron and dangling-bond signal, as these lines are close in *g* value and linewidth, and thus difficult to resolve separately. A potential negative LESR signal of the DB, for instance, will introduce an error with a maximum underestimation in the derived electron-spin density given by the dark spin density N_s. The derived difference ΔN would then be overestimated by $c_1 N_s$. In the case of the annealed sample, with the assumption of a full negative dangling-bond LESR signal, we obtain a lower limit of $\Delta N_{\min} = \Delta N - c_1 N_s \sim 1.3\times10^{16}$ for the charged-defect density. Partial saturation of the DB line

at the temperatures and microwave powers where the LESR signals are recorded may decrease the error and so adds to the accuracy of the derived ΔN. A potentially positive LESR signal, on the other hand, will lead to an underestimation of the charged-defect density. In any case, the lowest density of charged defects in the annealed film consistent with the LESR results is 1.3×10^{16} cm^{-3}.

Although we cannot completely exclude the possibility of a negative DB LESR line, the width and g value of our data are quite accurate due to the extended averaging procedures. No evidence for an appreciable contribution to the LESR signal by dangling bonds is found, particularly for medium and high excitation conditions. For low excitation intensities, where n_s is comparable to the dark spin density, we did observe systematic changes in the line shape of the narrow line. In the case of the annealed sample, it was found that the g value of the narrow line shifts from ~2.0043 to ~2.0050 and the width increases from 5.5 G to about 7 G. But for those conditions we were not able to obtain a satisfactory fit with only two Gaussian lines. Assuming a third Gaussian line of width 7.5 G and $g=2.0055$, good fits are achieved when 50–70 % of the narrow component is assigned to the DB line, indicating a positive LESR signal of the dangling bonds, and 30–50 % to the e line at $g=2.0043$. An example for an extensively averaged LESR signal at 165 K is shown together with the fits in Fig. 6. Of course, some ambiguity exists in splitting the intensity between the DB and e line, but additional confirmation was obtained from microwave saturation of the DB line. At 165 K, the h line and particularly the e line saturate at considerably higher microwave power than the DB line.[18] The combined LESR line shape, measured under different microwave powers, could be fitted by adjusting only the DB line according to the independently measured saturation of the DB in the dark and leaving all other parameters constant.

We emphasize that at low n_s the annealed sample shows a *positive* LESR signature of the DB line with a density of $2.1-2.6\times10^{15}$ cm^{-3}, corresponding to an *increase* of the DB density by 60–80 % of the dark spin density. Even up to room temperature, extended averaging shows a positive LESR signal of width 10–11 G and g value of 2.0065–2.007, with an integrated absorption of 30–50 % of the dark spin density. However, due to the high noise level and increasing overlap of the h and DB lines, a decomposition into single components would not be unique. The important point is that the DB LESR signal is positive rather than negative as expected if in the dark all defects were neutral.

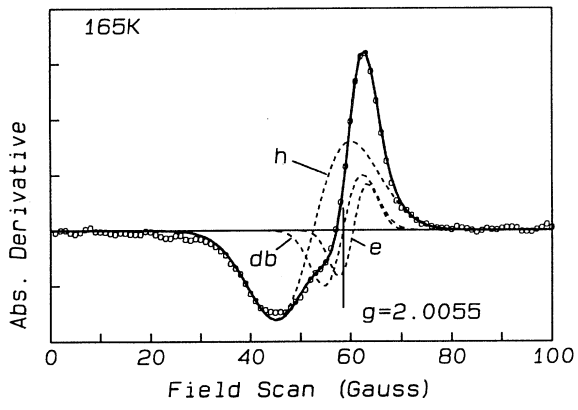

FIG. 6. LESR spectra at 165 K (microwave power is 0.5 mW) and fit by three Gaussian lines. Details in the text.

In Figs. 3 and 5 one data point is shown with an arrow. The point indicates the upper limit of n_t under the assumption that no DB line is present, and the arrow gives the range of n_t and p_t-n_t assuming that part of the narrow component in the LESR signal is due to a positive DB signature, as derived in Fig. 6. It is clear that the evidence for charged defects remains regardless of the effect of a DB LESR signal.

E. Dependence on film thickness and absorption profile

The most extensive data regarding intensity and temperature dependence were collected from the 15-μm-thick sample, but data from ~5-μm thick films showed a similar lack of proportionality between the electron and hole density, although to a somewhat lesser extent. The question remains whether this effect in fact is a true bulk response of the material or due to some interface or surface-related states. We addressed this point in two ways: first, by comparing the results of the thick sample with data from very thin samples that have a dominant fraction of surface or interface states, and second, by studying the effect as a function of light-absorption profiles in the thick sample.

Consider first the 0.3-μm-thick film. Under the highest available white light excitation we obtained a hole areal density of 3.9×10^{13} cm^{-2} in combination with an electron-spin areal density of 1.6×10^{13} cm^{-2}. Assuming the same proportionality constant that relates electron-spin density to total electron density as for the thicker films, $c_1(32\ K)=2.3$, the maximum density of negatively charge defects ΔN is 3×10^{12} cm^{-2} or 9×10^{16} cm^{-3}, which gives a ratio of charged to neutral defects around 1.3. Similar values $\Delta N=4-9\times10^{16}$ cm^{-3} were obtained for lower excitation intensity. The numbers for the dark spin density and charged-defect density and corresponding ratios of charged-to-neutral defects compare within a factor of 2 to those of the degraded thick sample, suggesting that the interface/surface defect structure is similar to the degraded bulk structure. The same conclusion may be drawn from the fact that this highly defective interface region does not respond to light soaking as much as the thick sample does. Extended light soaking to saturation of the thin sample increased the dark spin density only by a factor 3 compared to more than a factor 10 achieved for the thick sample.

Under white light excitation, for a given excitation intensity the absolute LESR signal of the 0.3-μm film is a factor 10 and the difference between hole and electron signal a factor 15 smaller than that of the 15-μm film, and for red light excitation, the LESR signal is approximately proportional to the film thickness, ensuring that the data

from the thick film indeed reflect the bulk properties of the defect structure. Further confirmation for this is obtained by varying the absorption profiles in the thick film. For a given excitation intensity, white light largely absorbed within the first few 100 nm from the sample surface produced the same LESR signature, with the disproportionality between holes and electrons, as red light that was adjusted to give a nearly homogeneous absorption profile across the sample thickness, indicating a homogeneous density of charged defects throughout the film. Also, LESR signatures of films deposited on Cr-coated substrates were identical with signatures of samples on SiO_2, and white light excitation produced the same signal for the case of illumination through the top surface as for the case of illumination through the substrate, showing no discernible difference for the contribution of top surface, quartz interface, or Cr interface layers to the signal.

F. Defect structure

From our LESR measurements, we have established a difference between band-tail hole and band-tail electron density, $p_t - n_t$, which, in annealed or as-grown material, if a factor 5–10 larger than the neutral dangling-bond density. To maintain charge neutrality, this difference must be balanced by defects or impurities that become negatively charged under illumination, N_{D^-}, so that $N_{D^-} = p_t - n_t$.

We further can estimate the range of energy positions where the associated defect states are placed in the gap. First, in order to pick up charge under illumination, these states must lie between the quasi-Fermi levels. In particular, they must be lower in energy than the deep conduction-band tail, as their recharging is observed for an electron occupation of the tail as low as $n_t = 10^{15}$ cm^{-3}. This rules out shallow n-type-doping impurities as the origin of these defect states. Second, as they are not detected in dark ESR and hence must be positively charged in dark equilibrium, these states must lie above the dark Fermi level. Therefore, an explanation of the LESR data essentially requires the presence of a band of positively charged defects in the range 0.4–0.7 eV below the conduction-band edge.

To maintain charge neutrality in the dark, these positively charged defects must be balanced by negatively charged defects or impurities below E_f. No further constraints are placed on the energy position of the states below E_f, and in principle our LESR results might be expected for slightly p-type-doped material. However, the Fermi level of our thick samples is ~ 0.7 eV below the conduction-band edge, in the upper half of the gap, and somewhat closer to E_c than observed in thinner samples, which makes p-type impurity doping highly unlikely. In addition, p-type-doped a-Si:H usually shows a clear positive LESR signal of the DB line,[19] which was not observed in our samples. These considerations suggest that the two charged defect bands are intrinsic to the bulk of undoped a-Si:H.

III. OCCUPANCY CALCULATIONS

Our results have indicated that band-to-band excitation leads primarily to double occupancy of the deep defect states explaining the lack of a positive LESR signature of deep defects in spite of the rather high density of charged defects that are present in the dark. However, the question why under illumination these defects become negatively charged instead of neutral immediately arises. If charged defects generally show larger capture coefficients for free carriers than the neutral ones, one would expect that under illumination the majority of deep defects would be neutral, a result not observed.

It is illustrative to have a closer look at the nonequilibrium steady-state occupancy functions of the dangling bond, f^+ (zero occupancy), f^- (double occupancy), and f^0 (single occupancy) under illumination. From detailed balance one obtains for the case of single occupancy[20]

$$f^0(E,n,p) = \frac{1}{1 + \dfrac{e_n^0 + pc_p^0}{e_p^+ + nc_n^+} + \dfrac{e_p^0 + nc_n^0}{e_n^- + pc_p^-}} , \tag{2}$$

where e_n^0, e_p^0, e_n^-, and e_p^+ are the emission coefficients of electrons and holes from charged and neutral traps, and c_n^0, c_p^0, c_p^-, and c_n^+ are the associated capture coefficients. If the defect states in question lie between the two quasi-Fermi levels for electrons and holes, the reemission processes may be neglected and the above equation is approximated as

$$f^0(E,n,p) = \frac{1}{1 + \dfrac{pc_p^0}{nc_n^+} + \dfrac{nc_n^0}{pc_p^-}} . \tag{3}$$

It is immediately apparent that f^0 strongly depends on the ratio of free electrons to holes and associated capture rates. f^0 is close to 1 only if both factors in the denominator are much smaller than 1, i.e., $c_n^+ / c_p^0 \gg p/n$ and $c_p^- / c_n^0 \gg n/p$. For undoped films it is known that under illumination $n/p \approx 10$, derived, for instance, from steady-state $\mu\tau$ products.[21] Then the critical requirement for $f^0 \approx 1$ is $c_p^- / c_n^0 \gg 10$. Experimental data for the various capture rates are available from transient $\mu\tau$ measurements[22] and yield

$$\frac{c_p^-}{c_n^0} = \frac{\mu_{0,p}}{\mu_{0,n}} \frac{(\mu\tau N_s)_{e \to D_0}}{(\mu\tau N_s)_{h \to D_-}} \approx 1.7$$

for extended state mobilities $\mu_{0,n} = 10\mu_{0,p}$ and the values of $\mu\tau N_s$ given in Ref. 22. From steady-state double injection measurements[23] one find $c_p^- / c_n^0 \approx 0.27$. Both values are much smaller than 10 and with those we obtain a rather low probability for single occupancy $f^0 \approx 0.03$-0.15, consistent with the absence of a large positive LESR signature of the dangling bond. Similarly, with the appropriate expressions for f^+ and f^- we find $f^+ < 0.01$ and $f^- = 0.85$-1, confirming our results that under strong illumination most deep defects will be doubly occupied.

For medium excitation intensities, the reemission terms may not be neglected and the situation is somewhat

more complex. Using a simple recombination model of defects with two correlated transition levels in the gap, we can numerically calculate the steady-state occupancy of defects and tail states as a function of generation rate. The program we used can handle an arbitrary continuous distribution of gap states $D(E)$ with correlated transition levels and tail states $N_{ct}(E)$ and $N_{vt}(E)$. The solution follows the procedure given in Ref. 20: Charge neutrality requires

$$n+n_t+N_{D^-}=p+p_t+N_{D^+} , \tag{4}$$

where

$$n_t=\int N_{ct}(E)f_t(E,n,p)dE ,$$

$$p_t=\int N_{vt}(E)[1-f_t(E,n,p)]dE ,$$

$$N_{D^-}=\int D(E)f^-(E,n,p)dE ,$$

$$N_{D^+}=\int D(E)f^+(E,n,p)dE ,$$

and f_t, f^+, and f^- are given in Ref. 23. Equation (4) yields a parametric expression for n and p, and for given capture rates we may calculate n, p, n_t, p_t, N_{D^-}, N_{D^+}, and N_{D^0} as a function of generation rate.

To be specific, for the calculations we have assumed typical values of 25 and 45 meV for the exponential conduction- and valence-band-tail slopes and two alternative distributions for the defect states. The first is a single, dominant defect band with a comparatively large effective correlation energy of 0.4 eV, in the following called the standard defect model. With this structure, in dark equilibrium most defects are singly occupied. The second defect distribution shows a center band in combination with two dominant side bands and a relatively small correlation energy of 0.12 eV (the defect pool distribution[2–5]). Both distributions with their associated $D^{+/0}$ and $D^{0/-}$ transition levels are shown in Fig. 7. Both distributions have been calculated using a specific defect equilibration model where[3]

$$D(E)=\gamma P(E)\left[\frac{1}{f^0(E)_{/\text{dark}}}\right]T_{\text{eq}}/2T_v . \tag{5}$$

$D(E)$ is the resulting one-electron density of states, $P(E)$ is the statistical energy distribution of available defect sites, assumed to be Gaussian, T_{eq} is the equilibration temperature, T_v is the exponential valence-band-tail parameter, and γ is adjusted to give the measured dark spin density of 3×10^{15} cm^{-3}. A typical rms width of $P(E)$ of 150 meV in combination with $U_{\text{eff}}=0.4$ eV yields the defect distribution of Fig. 7(a), and a width of 160 meV in combination with $U_{\text{eff}}=0.12$ eV yields the defect structure in Fig. 7(b). Equilibrium occupation statistics yields a comparatively small ratio of 1:2 for the charged-to-neutral defect density in the case of the standard model Fig. 7(a) and a ratio of 8:1 in the case of the defect pool distribution, the latter in accordance with our requirements from LESR results. It is important to emphasize that both cases have the same number of free parameters (3) that determine the density of states, i.e., pool position, pool width, and correlation energy. These have been selected such that the Fermi energy is 0.7 eV below the conduction-band edge and the dominant defect levels are located at 0.5 and 0.9 eV below the conduction-band edge, consistent with many experimental observations.[24] The main parameter leading to the different density of states in Figs. 7(a) and 7(b) is the assumed correlation energy.

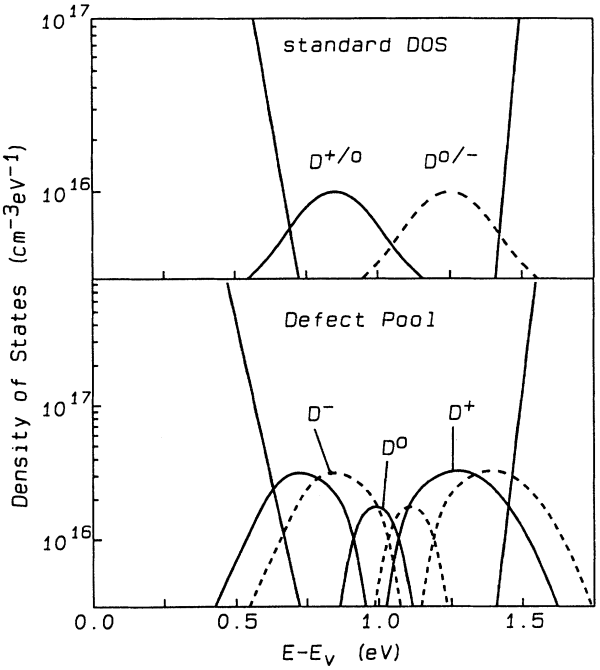

FIG. 7. Model density of states in the band gap according to the standard and defect pool model. Full curves correspond to $D^{+/0}$ and dashed curves correspond to $D^{0/-}$ transitions, shifted by the assumed correlation energies of 0.4 and 0.12 eV, respectively. In the case of the defect pool DOS, the total DOS is shown separated into actual equilibrium occupancy bands D^-, D^0, and D^+ at 300 K.

Figure 8 shows the various occupation densities as a function of generation rate. The figure provides a number of interesting observations. Over the whole range of generation rates, we find $n \gg p$, largely a result of the asymmetric tail-state distributions. Due to the steep slope of the conduction-band tail, n_t follows closely the free-electron density n, being about a factor 10 larger than n. Because of the much broader valence-band tail, p_t is some orders of magnitude higher than p, but increases slower than p with generation rate. At high excitation rates, n_t approaches p_t, satisfying charge neutrality in this regime. At medium generation rates, however, the charge balance is dominated by p_t and N_{D^-}, and the transition between the two regimes shows the disproportionality between n_t and p_t as observed in LESR. At low intensities, the charge balance is dominated by N_{D^-} and N_{D^+}. But over the whole range N_{D^0} does not change appreciably, consistent with the negligible LESR signal of the DB.

The change of N_{D^0} with generation rate is more clearly

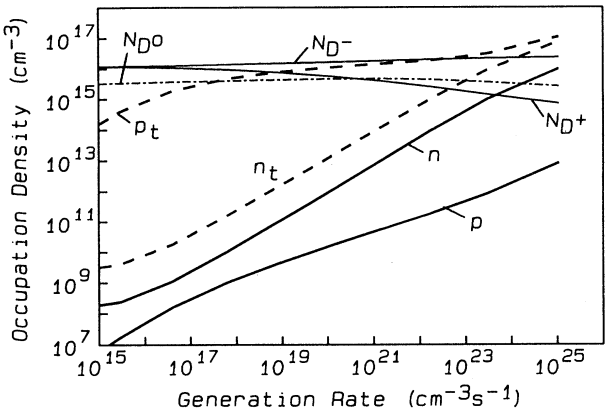

FIG. 8. Densities of free carriers, carriers in tail states, and positive, negative, and neutral defects under illumination at 300 K, calculated for the defect pool DOS of Fig. 7(b), and with capture rates from Ref. 23.

displayed in Fig. 9 for two defect distributions in Fig. 7 and for various capture rates. We find, even for symmetrical capture rates and a factor 10 difference between capture into neutral and into charged defects (curve *a*) that the maximum increase of spin density with illumination is only a factor 2.3, much smaller than the factor 8 between charged and neutral defect densities. For realistic capture rates (curves *b* and *c*) an increase to 1.5 times the dark spin density is found, in good agreement with our data at 165 K (Fig. 6). These values decrease further if defect pool structures with smaller charged-to-neutral ratios are used in the calculations. On the other hand, with the standard model a *drop* of spin density under illumination, even for rather low generation rates, is obtained, in contrast to experimental observations, and the curves were found to be insensitive to the exact values of the capture rates, provided that the rates into charged defects are not more than a factor 10 higher than into neutral ones.

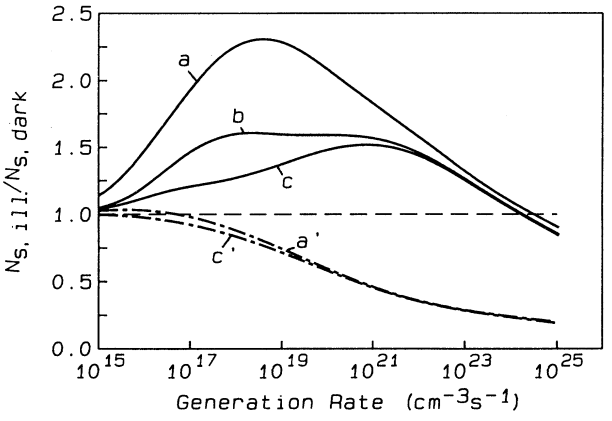

FIG. 9. Calculated change of spin density with illumination. Curves *a*–*c*, defect pool DOS; *a'*–*c'* standard DOS. (a) $c_n^+ = c_p^- = 10c_n^0 = 10c_p^0$. (b) Capture rates from $\mu\tau$ measurements (Ref. 22). (c) Capture rates from double injection experiments (Ref. 23).

Although the occupancy calculations were carried out for room temperature, the same general features should be expected for lower temperatures, provided that the ratios of the associated capture rates in Eqs. (2) and (3) do not change drastically with temperature. For temperature-independent capture rates or if all rates obey the same temperature dependence, changing the temperature will only shift all curves to higher or lower generation rates.

IV. DISCUSSION

With LESR, a band-tail hole density is observed which, at sufficiently low excitation intensities, is significantly larger than the band-tail electron density. The difference $\Delta N = p_t - n_t$ is derived using the *deviation* from proportionality at low excitation intensities, with the assumption that at high intensities electron and hole densities are equal. The derived values for ΔN do not rely on any absolute numbers obtained for the measured electron-spin densities and do not depend on any particular mechanism that may be responsible for the discrepancy between total electron density and apparent electron-spin density. The derived ratio of charged to neutral defects $\Delta N/N_s$ does not depend on the absolute calibration of the ESR setup and relies only on two assumptions: (i) the measured band-tail hole spin density is identical to the total hole density (no spin pairing, no saturation effects), and (ii) the factor c_1, relating electron spin density to the total band-tail electron density, is independent of n_s within the covered range of electron-spin densities. Spin pairing of band-tail holes can be ruled out (Stuke), care was taken to avoid saturation of the hole line, and the arguments given in Sec. III C make an intensity dependence of c_1 very unlikely. By extended averaging and by exploiting the different saturation behavior for the *e* and DB line, we were able to separate contributions from dangling bonds and electrons to the narrow (*e*+DB) line. But even neglecting that and assuming the most unfavorable situation of a full negative DB LESR signature, a lower limit for $\Delta N/N_s \approx 5$ was obtained for the bulk defect structure of low defect *a*-Si:H.

We would like to relate our results to other experiments in this field. As already mentioned, earlier LESR studies indicated a ratio of roughly 1:1 for tail-state electron-to-hole density under high excitation levels and band-to-band excitation.[6,11] We have reexamined and deconvoluted those spectra and indeed obtained a best fit for an electron-to-hole ratio of around 1:2.5, in agreement with our present results and recent results from other groups.[25] Of course, accounting for the spin coupling of tail-state electrons, the original conclusion with a ratio of 1:1 for all tail-state electrons to holes is approximately valid for high excitation where $p_t, n_t \gg p_t - n_t$, and only for lower excitation does the deviation from proportionality become apparent.

Under ir-excitation an *increase* of the electron line with respect to the hole line was observed,[11] suggesting the presence of *positively* charged defects under illumination

to balance the excess electron density. On the other hand, our results show a *smaller* electron than hole density under low band-to-band excitation, indicating the presence of additional *negatively* charged defects. In agreement with our results, a decrease of the narrow line with respect to the hole line was found after light soaking,[12] although no dependence on excitation intensity was reported. The ir results on different types of samples suggested an interface effect, and one possibility to generate charged defects near interfaces could be band bending towards the interface. Our results, on the other hand, proved to be a clear bulk response, independent of film thickness, absorption profile, and substrate material. In fact, for thinner films whose dark spin density is dominated by the interface layer, the density of charged defects under illumination is not much higher than the dark spin density. This may mask the true bulk response of device-grade material up to film thicknesses of several micrometers. Apart from the interface vs bulk issue, however, the ir results do not essentially contradict our findings. With the two bands of negatively and positively charged defects present, band-to-band excitation by subsequent trapping processes apparently leads to negative charging of those defects that are unoccupied in the dark while subgap illumination may preferably excite electrons out of the doubly occupied defect band and so lead to a net excess of positively charged defect states.

Subgap absorption shows a distinct deviation from dark spin density for larger film thicknesses,[10] indicating a higher ratio of charged to neutral defect density in the bulk than close to the surface or interface, in good agreement with the present LESR results. A significant difference between surface and bulk microstructure with larger correlation energies for surface-related defects was inferred from the temperature dependence of the dark spin density.[26] Larger correlation energies, however, should lead to a lower ratio of charged to neutral defects, again supporting our results regarding the dependence of LESR on film thickness. With light soaking, an increase in subgap absorption was observed,[9] which was, by a factor ~ 2.5, smaller than the corresponding increase in spin density for film thicknesses ≥ 15 μm, again in quantitative agreement with the LESR data. Both results indicate that the observed proportionality[7] of subgap absorption and spin density derived for high defect densities is not valid for the bulk defect structure of undoped low defect *a*-Si:H. Our results on sufficiently thin films and light-soaked films suggest that the matrix element linking defect density to optical absorption should be larger by a factor ~ 2 than originally proposed[7] to account for the additional charged defects present in light-soaked or thin samples. Together with the deviations between ESR and subgap absorption on thick, annealed films, this yields for the bulk defect structure of annealed films 5–10 times more charged than neutral defects.

While the input parameters for occupancy calculations, such as tail state distribution, bandgap, or effective density of states at the mobility edges, do influence the quantitative features of Fig. 8 to some extent, the occupation functions f^0, f^+, and f^- show little dependence on these parameters, provided that the calculations yield (as required by experiment[21] a free-electron density $n > p$ over the range of generation rates. Hence, assuming that the experimentally derived capture rates[22,23] are reasonable, the observed small positive LESR signal of the DB requires a density of charged DB's well in excess of neutral DB's in undoped *a*-Si:H. In fact, if we would assume that in the dark no appreciable fraction of charged defects was present, with the values of f^0 derived in Sec. III we should expect a large negative LESR signal of the dangling-bond under illumination, starting already at relatively low generation rates at room temperature, a behavior that has never been observed. As shown in detail by Vaillant and Jousse, for such a defect structure a small or negligible LESR signal is only expected if the capture rates of charged DB's are much larger (≈ 50) than those of neutral DB's, and if capture rates for electrons and holes are symmetrical, both assumptions that are not in agreement with the experimental data.[22,23]

An additional complication may be present for typical films of thickness around 1 μm, which have an appreciable or dominant contribution of interface defects. In such a case, due to the high recombination rates at the defective interface, the occupation of those states may not change appreciably, and hence quench any positive or negative dangling-bond LESR signature on those samples further.

The recombination model to calculate the various occupancies in Fig. 8 has been previously applied to predict the dependence of steady-state $\mu\tau$ products on temperature and Fermi level, based on the two alternative defect structures of Figs. 7(a) and 7(b).[24] The results were incompatible with the standard defect model and favored a defect structure according to the defect pool model, in agreement with our present results. We conclude that in undoped equilibrated *a*-Si:H electronic properties as well as defect occupancies observed by LESR, at least for steady-state conditions, are consistently and better explained by a defect structure containing a dominant fraction of charged dangling bonds. Less understood are electronic properties of *a*-Si:H inferred from transient behavior. Recent results on trap filling dynamics have been interpreted as relaxation processes associated with capture into deep defects.[27] Transient $\mu\tau$ and charge collection measurements suggest much lower defect densities[28] than deduced from the present LESR experiment, but the correlation between defect density and transient $\mu\tau$ products on which these results are based seems controversial.[29]

V. CONCLUSIONS

Our LESR measurements have shown a distinct deviation from proportionality between band-tail electron and hole density as well as a small positive LESR signature of the DB line in the bulk of undoped low defect *a*-Si:H. The results suggest a density of charged DB's which is at least a factor 5 higher than the density of neutral DB's. Occupancy calculations confirmed that under illumination most DB's become negatively charged, and therefore no appreciable positive LESR signature of the DB line is expected, even for a dominant fraction of charged DB's

present in the dark.

Because the defect structure of the interfaces is different from the bulk and the interface defects dominate the spin signal for films up to 5 μm, an unambiguous observation of this effect requires a minimum film thickness of more than 5 μm. However, many electronic properties are dominated by the bulk defect structure with little influence of the interface even for comparatively thin samples. This may explain many apparent inconsistencies between properties derived from electronic measurements and derived from ESR or LESR.

Although the so-called defect pool model has been of considerable success in explaining defect densities and defect distributions of doped material[30,31] and has been applied to describe metastable changes in thin-film transistors,[32] the understanding of the bulk defect structure of undoped material suffered from the above-mentioned inconsistencies. With our measurements and occupancy calculations, we have demonstrated that ESR and LESR results are consistent with the predictions of the defect pool model. In this framework the defect structure of intrinsic material may be viewed as a smooth transition from *n*- to *p*-type *a*-Si:H, where the two charged-defect bands observed in doped material are of approximately equal density. Correlations observed between spin density and electronic properties, which generally have been taken as indication for the neutral dangling bond being the main recombination center, are in fact due to correlations between the charged and neutral defect densities as a result of equilibration. On the other hand, deviations from straight proportionality[14] are consistently explained by changes in the ratio of charged to neutral defect densities under conditions such as light soaking.

ACKNOWLEDGMENTS

We wish to thank M. Brandt and M. Stutzmann for several discussions, and C. C. Tsai for supplying the *a*-Si:H specimens. Support by NREL under Contract No. HG-1-10063-9 is gratefully acknowledged.

[1]Y. Bar-Yam, D. Adler, and J. D. Joannopoulos, Phys. Rev. Lett. **57**, 467 (1986).
[2]G. Schumm and G. H. Bauer, Philos. Mag. B **64**, 515 (1991).
[3]G. Schumm and G. H. Bauer, J. Non-Cryst. Solids **137/138**, 315 (1991).
[4]S. C. Deane and M. J. Powell, Phys. Rev. Lett. **70**, 1654 (1993).
[5]H. M. Branz and M. Silver, Phys. Rev. B **42**, 7420 (1990).
[6]R. A. Street and D. K. Biegelsen, Solid State Commun. **33**, 1159 (1980).
[7]W. B. Jackson and N. M. Amer, Phys. Rev. B **25**, 5559 (1982).
[8]M. Stutzmann and W. B. Jackson, Solid State Commun. **62**, 153 (1987).
[9]G. Schumm, E. Lotter, and G. H. Bauer, Appl. Phys. Lett. **60**, 3262 (1992).
[10]M. Favre, A. Shah, J. Hubin, E. Bustarret, M. A. Hachicha, and S. Basrour, J. Non-Cryst. Solids **137/138**, 335 (1991).
[11]J. Ristein, J. Hautala, and P. C. Taylor, Phys. Rev. B **40**, 88 (1989).
[12]Z. M. Saleh, H. Tarui, K. Ninomiya, T. Takahama, Y. Nakashima, N. Nakamura, H. Haku, K. Wakisaka, M. Tanaka, S. Tsuda, S. Nakano, Y. Kishi, and Y. Kuwano, Jpn. J. Appl. Phys. **31**, 995 (1992).
[13]T. Shimizu, H. Kidoh, A. Morimoto, and M. Kumeda, Jpn. J. Appl. Phys. **28**, 586 (1989).
[14]S. Guha and M. Hack, J. Appl. Phys. **58**, 1683 (1985).
[15]S. Hasegawa, J. Kasajima, and T. Shimizu, Philos. Mag. B **43**, 149 (1981).
[16]H. Dersch, J. Stuke, and J. Beichler, Phys. Status Solidi B **107**, 307 (1981).
[17]M. Stutzmann, D. K. Biegelsen, and R. A. Street, Phys. Rev. B **35**, 5666 (1987).
[18]M. Stutzmann and D. K. Biegelsen, Phys. Rev. B **28**, 6256 (1983).
[19]R. Carius and W. Fuhs, J. Non-Cryst. Solids **77/78**, 659 (1985).
[20]F. Vaillant and D. Jousse, Phys. Rev. B **34**, 4088 (1986).
[21]J. Koçka, C. E. Nebel, and C.-D. Abel, Philos. Mag. B **63**, 221 (1991).
[22]R. A. Street, Philos. Mag. B **49**, L15 (1984).
[23]A. Doghmane and W. E. Spear, Philos. Mag. B **53**, 463 (1986).
[24]G. Schumm, C.-D. Abel, and G. H. Bauer, J. Non-Cryst. Solids **137/138**, 351 (1991).
[25]R. Saleh, I. Ulber, and W. Fuhs, in *Amorphous Silicon Technology—1993*, edited by E. A. Schiff, M. F. Thompson, P. G. LeComber, A. Madan, and K. Tanaka, MRS Symposia Proceedings No. 297 (Materials Research Society, Pittsburgh, in press).
[26]J.-K. Lee and E. A. Schiff, Phys. Rev. Lett. **68**, 2972 (1992).
[27]J. D. Cohen, T. M. Leen, and R. J. Rassmussen, Phys. Rev. Lett. **69**, 3358 (1992).
[28]R. A. Street, J. Zesch, and M. J. Thompson, Appl. Phys. Lett. **43**, 672 (1983).
[29]N. Beck, N. Wyrsch, E. Sauvain, and A. Shah, in *Silicon Technology—1993* (Ref. 25).
[30]K. Winer, Phys. Rev. B **41**, 12 150 (1990).
[31]K. Pierz, W. Fuhs, and H. Mell, Philos. Mag. B **63**, 123 (1991).
[32]M. J. Powell, C. van Berkel, and S. C. Deane, J. Non-Cryst. Solids **137/138**, 1215 (1991).